AMERICAN JOURNAL of PHYSICS

A Journal Devoted to the Instructional and Cultural Aspects of Physical Science

VOLUME 35, NUMBER 7 JULY 1967

Measurement of Atomic Lifetimes by the Hanle Effect*

R. L. DEZAFRA AND W. KIRK
State University of New York, Stony Brook, New York
(Received 21 September 1966; revision received 27 February 1967)

An experiment is described which utilizes the Hanle technique for measurement of atomic excited-state lifetimes, with particular application to the $^3P_1$ state of mercury. The components for the experiment are comparatively inexpensive or readily constructed, and the technique is one of the few which directly illustrate features of the interaction between radiation and free atoms. A simple classical description of the effect is given, followed by a more detailed quantum description, as well as constructional details of an experimental arrangement suitable for an advanced undergraduate or graduate laboratory.

I. INTRODUCTION

A VARIETY of techniques are available for the measurement of atomic excited-state lifetimes,[1] but few are as elegant and simple as the technique discovered by Hanle in the 1920's.[2] Hanle's technique, for all its accuracy and simplicity, was largely unexploited and generally forgotten until recent years, perhaps owing chiefly to observational difficulties in the days before photomultiplier tubes became commercially available. In 1959, Colegrave, Franken, Lewis, and Sands[3] rediscovered experimentally the "level-crossing" technique theoretically explored in the 1930's by Breit[4]; and with this came a rediscovery of the Hanle effect, which is nothing more than a special case of level-crossing degeneracy at zero magnetic field. (The levels referred to here are the Zeeman magnetic sublevels of the fine or hyperfine energy levels in a magnetic field.) Recently, a number of lifetime measurements have been made with good precision using the Hanle technique,[5] and these determinations are probably the most reliable in the literature of lifetime measurements. The reasons for this are twofold: the Hanle technique does not require a direct knowledge of the vapor density of the atoms whose excited-state lifetimes are being measured, a requirement which has led to systematic errors in other techniques such as the "hook method"[1]; and secondly, it is particularly effective for lifetimes in the 10^{-8}–10^{-9}-sec range, where other techniques also independent of vapor pressure begin to lose their accuracy.

* This work supported in part by a National Science Foundation grant.

[1] For example, A. C. Mitchell and M. W. Zemansky, *Resonance Radiation and Excited Atoms* (Cambridge University Press, New York, 1961), p. 145; E. W. Foster, Rept. Progr. Phys. 27, 469 (1964); W. R. Bennett, Jr., P. J. Kindlmann, and G. N. Mercer, Appl. Opt., Suppl. 2, 34 (1965).

[2] W. Hanle, Z. Physik 30, 93 (1924); Ergeb. Exakt. Naturwiss. 4, 214 (1925). Also, Ref. 1, Chap. V.

[3] F. D. Colegrove, P. A. Franken, R. R. Lewis, and R. H. Sands, Phys. Rev. Letters 3, 420 (1959).

[4] G. Breit, Rev. Mod. Phys. 5, 91 (1933).

[5] For example, A. Lurio and R. Novick, Phys. Rev. 134, A608 (1964); A. Lurio, R. L. deZafra, and R. J. Goshen, *ibid.*, p. A1198; A. Landman and R. Novick, *ibid.*, p. A56; D. K. Anderson, *ibid.* 137, A21 (1965); A. Lurio, *ibid.* 140, A1505 (1965); B. Budick, Bull. Am. Phys. Soc. 10, 1096, 1214 (1965); W. W. Smith and A. Gallagher, Phys. Rev. 145, 26 (1966); A. Gallagher and A. Lurio, *ibid.* 136, A87 (1964).

The Hanle technique does suffer from two drawbacks, both of which are shared in common with some other lifetime measuring techniques. The first of these is caused by "coherent trapping" of radiation in the absorbing vapor; the other is caused by nonuniformities in the intensity profile of the resonance lamp line used to excite the atomic levels under study. Methods for limiting or eliminating these drawbacks are discussed in detail below.

A Hanle-effect experiment is attractive for a teaching laboratory for several reasons: It is comparatively inexpensive and simple to set up; it is a "live" technique being used in current research, it is illustrative of indirect techniques of time measurement used not only in atomic but nuclear lifetime studies; the experiment can be performed on various levels of sophistication, employing either semiclassical or quantum analysis; and finally, it is one of a relatively few feasible experiments directly illustrating features of the interaction between radiation and free atoms. The theory and experiment described in the remainder of this paper would be suitable for an advanced undergraduate or a graduate laboratory. A simplified version could be carried through in one or two 3-h periods—a more thorough approach might take four to six 3-h periods.

I. THEORY OF THE EXPERIMENT

A. Semiclassical Approach

Consider a lamp producing radiation from a particular transition in some atomic species. Let this light be polarized in the horizontal (x–y) plane by a linear polarizer as in Fig. 1. If a vapor

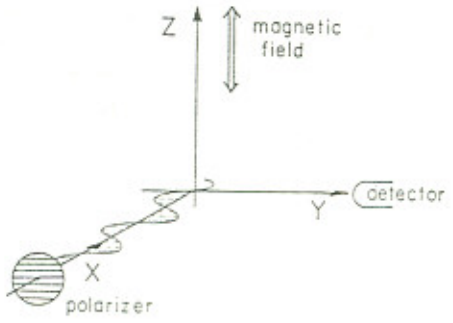

FIG. 1. Typical geometrical arrangement for a Hanle-effect experiment.

of atoms of the same species is located at the origin of the coordinate system (e.g., in a sealed bulb or in an atomic beam), these atoms will resonantly absorb and reradiate light of the same frequency—i.e., the light will be resonantly "scattered." Considering the absorbing atoms as classical dipoles set into oscillation along the y axis by the incident radiation, one sees by reference to Fig. 1 that no scattered radiation should be observed along the $\pm y$ axes, with the incident polarization as shown. On the other hand, if a magnetic field is present along the z axis, the dipoles excited by the radiation will precess about the field at the Lamor precession frequency ω_L. This frequency depends on the magnetic field H via the relation $\omega_L = \gamma H$ where γ is the gyromagnetic ratio, given in this case by

$$\gamma = \omega_L/H = g_J\mu_o/\hbar. \qquad (1)$$

with g_J being the electronic g factor for the excited state and μ_o is the Bohr magneton.

To determine the radiation intensity observed along the $+y$ axis in the case where a precession-causing magnetic field is present, we proceed as follows: The dipole radiation pattern in the x–y plane is determined by the familiar $\sin^2\theta$ term, where here θ would be measured with the y axis as reference. If the dipole is precessing at angular frequency ω_L and the observer stays fixed (say looking towards the origin along the y axis), then θ is replaced by $\omega_L t$, where t is the time elapsed since excitation of the dipole. A damping term $e^{-t/\tau}$ must be included also, since the dipole is radiating energy, where τ represents the mean life of the state involved.[6] In addition, it is most convenient to use continual excitation and continual observation: Hence, the observed intensity will be the result of an integration from zero to infinity in time. We thus obtain

$$I = C\int_0^\infty e^{-t/\tau}\sin^2\omega_L t\,dt, \qquad (2)$$

where C is a constant of proportionality. Equation (2) represents a standard form of integral

[6] More properly speaking, in terms of a single atom, the classical dipole pattern is proportional to the probability for emission of a photon in different directions, and the damping term is proportional to the probability of emission as a function of time.

which, when evaluated, gives

$$I = (C/2\tau)\{1 - [1 + (2\gamma H\tau)^2]^{-1}\} \quad (3)$$

which is just an inverted Lorentzian line shape having intensity $I = 0$ at $H = 0$, and increasing symmetrically with positive or negative magnetic-field values to an asymptotic intensity of $I = C/2\tau$. The full width at half-maximum intensity is equal to $1/\gamma\tau$. If $H_{1/2}$ is the magnetic field required to reach the half-maximum point in scattered light intensity, then, by trivial substitution into Eqs. (1) and (3), one finds that

$$1/\tau = (2g_J \mu_o H_{1/2}/\hbar)\ \text{sec}^{-1}. \quad (4)$$

Hence, a simple measure of the width at half-maximum serves to establish the mean life τ of the radiating state in question.

Instead of using plane-polarized light, as considered above, one may also use unpolarized light, since this may be resolved into two orthogonal plane polarized beams. For the component parallel to the z axis, the scattered light intensity is independent of the applied magnetic field, since a dipole excited in such a way that its axis lies along the z axis will not precess. In practice, it is desirable to use plane-polarized light to eliminate this constant background contribution which is otherwise present. If a good plane polarizer is not available, however (e.g., for lines in the far ultraviolet), there may be no choice but unpolarized light.

One may, in fact, also choose different input and field axes—i.e., if the magnetic field lies along the *input* axis, with input and output axes orthogonal, it is not hard to see that one again gets the Hanle effect with an inverted Lorentzian line shape if the incoming light is linearly polarized in the plane of the input and output axes. For light polarized perpendicular to this plane, the signal will be a normal Lorentzian, peaking at *zero* field. Note that hence this geometry cannot be used with unpolarized input radiation, as the net result would be a constant output independent of field. It may be shown that with this geometry, and with the input linearly polarized at 45° with respect to the input-output plane, the result is a dispersion curve, with the distance between the positive and negative peaks given again by $\Delta H = 1/\gamma\tau$.

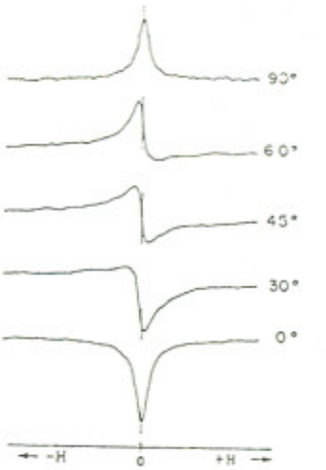

FIG. 2. Light intensity as a function of magnetic field from recorder tracings for various polarizer settings. In this case, the magnetic field was parallel to the input axis and the direction of observation was at right angles. The angular values refer to the position of the polarizer axis measured with respect to the plane defined by the input and output axes.

If an x–y recorder is available to speed the work, it is amusing to take a series of recordings of intensity vs field while rotating the polarizer through a series of positions from horizontal to vertical while using this geometry. See Fig. 2.

B. Quantum Description

The easiest point of departure for a quantum description is the Breit formula[4] (which has been rederived in a simplified approach by Franken[7]) for the rate at which light of polarization f is absorbed and light of polarization g is re-emitted by a free atom in a case of resonance fluorescence:

$$R(\mathrm{f},\mathrm{g}) = \text{const.} \sum_{\substack{\mu\mu' \\ mm'}} \frac{f_{\mu m} f_{m\mu'} g_{\mu' m'} g_{m'\mu}}{1 - i\tau(E_\mu - E_{\mu'})/\hbar} \quad (5)$$

where the constant is determined by the incident light intensity, the number of scattering atoms, geometrical factors, etc., m and m' refer to magnetic quantum numbers for Zeeman sublevels of the ground state; and μ, μ' refer similarly to sublevels of the excited state. E_μ is the energy of the μth excited substate. $f_{\mu m}$ and $g_{\mu m}$ are dipole transition-matrix elements between the states in question, given by

$$f_{\mu m} = \langle \alpha, J, \mu \,|\, \mathrm{f}\cdot\mathrm{r} \,|\, \alpha', J-1, m \rangle,$$
$$g_{\mu m} = \langle \alpha, J, \mu \,|\, \mathrm{g}\cdot\mathrm{r} \,|\, \alpha', J-1, m \rangle \quad (6)$$

[7] P. A. Franken, Phys. Rev. 121, 508 (1961).

for an initial state specified fully by the quantum numbers α, J, μ. r is a vector along the dipole axis.

In calculating the matrix elements, we note first that the selection rules for dipole transitions require that $\mu = m$, $m \pm 1$ only. [In our choice of notation for Eqs. (6), we have already anticipated dealing with a $J = 1$ excited-state $\rightarrow J = 0$ ground-state transition.] We further note that within the limits of the Zeeman effect to first order in H, $(E_\mu - E_{\mu-1}) = -(E_\mu - E_{\mu+1})$ and that $(E_\mu - E_{\mu-2}) = -(E_\mu - E_{\mu+2}) = 2(E_\mu - E_{\mu-1})$.

As a specific example, consider the intercombination transition $^1S_0 \leftrightarrow {}^3P_1$ in mercury. Here, for the ground and excited states, $J = 0, 1$ respectively, so that we have $m = m' = 0$ while values of μ, μ' range over $-1, 0, +1$. Nine terms thus enter into the sum in Eq. (5):

$$R = C \sum_{n=1}^{9} R_n = C \left\{ \begin{aligned} & f_{10}f_{01}g_{10}g_{01} + \frac{f_{10}f_{00}g_{00}g_{01}}{1 - i\tau\Delta E/\hbar} + \frac{f_{10}f_{0-1}g_{-10}g_{01}}{1 - i2\tau\Delta E/\hbar} \\ & + \frac{f_{00}f_{01}g_{10}g_{00}}{1 + i\tau\Delta E/\hbar} + f_{00}f_{00}g_{00}g_{00} + \frac{f_{00}f_{0-1}g_{-10}g_{00}}{1 - i\tau\Delta E/\hbar} \\ & + \frac{f_{-10}f_{01}g_{10}g_{0-1}}{1 + i2\tau\Delta E/\hbar} + \frac{f_{-10}f_{00}g_{00}g_{0-1}}{1 + i\tau\Delta E/\hbar} + f_{-10}f_{0-1}g_{-10}g_{0-1}, \end{aligned} \right. \tag{7}$$

where $\Delta E = (E_\mu - E_{\mu-1})$. To evaluate Eq. (7), the individual matrix elements of Eq. (6) are needed. These may be found in Condon and Shortley, for example,[8] and are, for the J and m values used here,

$$\begin{aligned} f_{0\pm1} &= \mp 1/2\sqrt{2}\,\mathbf{f}\cdot(\mathbf{i} \pm i\,\mathbf{j})\langle r\rangle = f_{\pm10}^{*} \\ f_{00} &= \mathbf{f}\cdot\mathbf{k}\,\langle r\rangle, \end{aligned} \tag{8}$$

with similar expressions for $g_{\mu m}$, where i, j, and k are unit vectors along the x, y, and z axes. f^* is the complex conjugate of f, and $\langle r\rangle$ is the reduced matrix element of r.

Now consider a component of incoming radiation directed along the x axis with its polarization vector f making an angle θ_1 with respect to the y axis, and a component of outgoing radiation directed along the y axis with its polarization vector g making an angle θ_2 with respect to the x axis. Then

$$\begin{aligned} \mathbf{f} &= \mathbf{j}\cos\theta_1 + \mathbf{k}\sin\theta_1, \\ \mathbf{g} &= \mathbf{i}\cos\theta_2 + \mathbf{k}\sin\theta_2. \end{aligned} \tag{9}$$

Equations (8) and (9) may now be substituted into (7) and the various terms regrouped to yield

$$\begin{aligned} R_{(\Delta\mu=0)} &= R_1 + R_5 + R_9 = \frac{1}{2}\cos^2\theta_1\cos^2\theta_2 \\ &\quad + \sin^2\theta_1\sin^2\theta_2, \\ R_{(\Delta\mu=1)} &= R_2 + R_4 + R_6 + R_8 \\ &= -\frac{i\cos\theta_1\sin\theta_1\cos\theta_2\sin\theta_2}{1 - i\tau\Delta E/\hbar} \\ &\quad + \frac{i\cos\theta_1\sin\theta_1\cos\theta_2\sin\theta_2}{1 + i\tau\Delta E/\hbar} \\ R_{(\Delta\mu=2)} &= R_3 + R_7 = -\frac{1}{4}\frac{\cos^2\theta_1\cos^2\theta_2}{1 - i2\tau\Delta E/\hbar} \\ &\quad - \frac{1}{4}\frac{\cos^2\theta_1\cos^2\theta_2}{1 + i2\tau\Delta E/\hbar}, \end{aligned} \tag{10}$$

where still the total rate

$$R(\mathbf{f}, \mathbf{g}) = \text{const.} \sum_{n=1}^{9} R_n.$$

Various experimental conditions now determine the final form of R (f, g). Thus, consider first the case where no polarization conditions are imposed on either the incoming or outgoing radiation. The θ_1 and θ_2 vary over all possible values, and $(\cos^2\theta_n)_{av} = (\sin^2\theta_n)_{av} = \frac{1}{2}$, while $(\cos\theta_n \sin\theta_n)_{av} = 0$. Hence,

$$R = \tfrac{1}{4}\,\text{const}\cdot\{1 - \tfrac{1}{2}[1 + (2\tau\Delta E/\hbar)^2]^{-1}\}. \tag{11}$$

For the case in which the input radiation is plane polarized in the xy plane and no polariza-

[8] E. U. Condon and G. H. Shortley, *The Theory of Atomic Spectra* (Cambridge University Press, New York, 1935, 1963), p. 63.

tion analysis is made of the outgoing radiation, $\theta_1 = 0$ and θ_2 again takes all possible values. One then obtains

$$R = \tfrac{1}{4}\,\text{const} \cdot \{1 - [1 + (2\tau\Delta E/\hbar)^2]^{-1}\}. \quad (12)$$

Remembering that $\Delta E = \hbar\omega$ and that $\omega = \gamma H$, Eqs. (11) and (12) are seen to be of the same form as Eq. (3), derived classically. Moreover, we see that (11) and (12) differ from each other only in that radiation is still scattered in the y direction when $\Delta E = 0$ (i.e., at zero magnetic field) in the first case—in fact with half the maximum possible intensity—but not in the second. This again was a feature predicted under the classical discussion for the two cases in which the incoming radiation is plane polarized or unpolarized.

The characteristic outputs of other geometrical arrangements, as discussed in Sec. A above, may be verified in the quantum approach by using the generalized treatment for arbitrary incident and output directions, and arbitrary polarization, as given in the paper by Lurio, deZafra, and Goshen cited in Ref. 5. However, one salient feature should be noted in the equations as worked out for the conditions discussed here: The $\Delta\mu = 0$ terms in Eq. (10) contribute only a constant (magnetic-field-independent) term. The $\Delta\mu = 1$ terms vanish, and the entire field-dependent effect comes from the $\Delta\mu = 2$ terms. These arise from the excited-state Zeeman sublevels differing from one another by 2 in the value of their magnetic quantum numbers.[9] In the case of a $J = 1$ system (e.g., the P_1 state of Hg or Cd), these are just the $\mu = \pm 1$ states, which go to the $m = 0$ ground state, whereas the $\Delta\mu = 0$ terms arise from the $\mu = 0 \rightarrow m = 0$ transition.

From a classical standpoint, it will be recalled that the normal Zeeman effect viewed at right angles to the field direction results in a central unshifted line which is plane polarized parallel to the field axis, and two satellite lines, each of half the intensity of the central line, shifted by $\pm$ the Larmor frequency from the central line, and plane polarized perpendicular to the field direction. These lines arise from the $\mu = 0 \rightarrow m = 0$ and $\mu = \pm 1 \rightarrow m = 0$ transitions, respectively. The presence of the unshifted line actually depends on whether or not dipole oscillations are excited with a component perpendicular to both the field and observing directions: In the usual Zeeman experiment (lamp in a magnetic field) this is so—this is also true in the first case [Eq. (11)] discussed above, due to the use of unpolarized input light, but not in the second [Eq. (12)]. We are thus led to conclude that, in the first case, the residual radiation observed at zero field corresponds to the unshifted central line in the normal Zeeman effect, and hence will be plane polarized along the magnetic field axis. The two frequency-shifted components, arising from the $\mu = \pm 1 \rightarrow m = 0$ transitions, contribute to the total radiation at nonzero field; but as the field is reduced to zero, the $\mu = \pm 1$ states will become degenerate and will thence radiate coherently. The phasing of this coherent emission is such as to give rise to destructive interference—thus these components vanish when viewed at zero field perpendicular to the field axis, and the intensity decreases.

It should be noted that the interference and coherence effects we are discussing here all involve the internal magnetic sublevels of a single given atom. These are *not* coherence and interference effects *between separate atoms connected by a common radiation bath*, as is the case in laser operation, for instance, or in the case of resonant trapping of radiation in a vapor of atoms, to be discussed below. The criterion for lifting of the degeneracy in magnetic substates is seen to be the requirement that $2\tau\Delta E/\hbar = 2\tau\omega_L$ be large as compared with unity—i.e., that the Zeeman splitting of the levels should be large compared with the natural width of the levels $\Delta E_{\text{nat.}} \simeq \hbar/\tau$.

It is evident that similar interference effects should occur not only at zero field but whenever sublevels differing by 2 in their magnetic quantum numbers can be made to cross by the application of a magnetic field. This is the well

[9] Note that this implies the impossibility of obtaining a Hanle effect with this geometry and polarization on any element in an excited state having $J < 1$, e.g., the $^2P_{1/2}$ excited states of the alkali doublets. Gallagher and Lurio have shown, however [Phys. Rev. Letters 10, 25 (1965)], that it is possible to obtain the Hanle effect in a $J = \frac{1}{2}$ state by using circularly polarized light and proper choice of geometry.

known "level-crossing" phenomenon discovered by Colegrove, Franken, Lewis, and Sands[3,7,10] and used recently for the measurement of numerous atomic and nuclear parameters.[11]

C. Effects of Lamp-Line Profiles and Coherent Trapping

In the theoretical treatments given above, it is implicit that the exciting lamp line is sufficiently broad in frequency spread to excite any of the Zeeman-split levels of the excited state with equal probability. With the low fields typically used for the Hanle effect ($\leq$ 50 G), the usual Doppler-broadened lamp lines are typically 10 to 100 times the Zeeman level spread.

Of more practical concern for the experiment described here is the process of "self-reversal" of a lamp line. This occurs when a cooler (relatively unexcited) outer layer of atoms absorbs radiation coming from deeper layers of the lamp vapor. The absorption occurs preferentially at the center of the Doppler-broadened line and can result in considerable loss of intensity at the line center. This in turn means that at zero field, the amount of scattered light from the resonance cell will be anomalously small. As the applied magnetic field increases, however, the Zeeman levels in the absorbing vapor of the cell move away from the nominal line-center energy and relatively more light is scattered in the wings of the Hanle signal. Experimentally, this will typically show up as a failure in ability to fit a Lorentzian line shape in the wings of the Hanle signal. The remedy lies in adjustment of lamp parameters (or even of the type of lamp) to minimize conditions leading to self-reversal, and/or placing the lamp in a magnetic field of at least several hundred gauss in order to produce Zeeman spreading and reduce the central self-absorption of the lamp line.

Although the resonance lines of mercury-vapor lamps are easily self-reversed, we have not found self-reversal to be an apparent problem with the $^3P_1 \rightarrow {}^1S_0$ intercombination line suggested for use, owing to its small oscillator strength. Self-reversal could be a problem in other cases—e.g., the $^1P_1 \rightarrow {}^1S_0$ transition in cadmium vapor, suggested as an alternative to the mercury experiment at the end of the next section. The condition to avoid is that of a centrally confined discharge column in the lamp vapor. Typically, an rf excited lamp will run in two or more modes, depending on how much power is fed to it, what frequency is used, at what temperature it is maintained, etc. By adjustment of these parameters, a mode should be sought in which the discharge is as uniform as possible throughout the lamp, or in which the outer layers are more strongly excited.

Coherent trapping, or, as it is often called, "coherence narrowing," is the second major phenomenon which can affect Hanle technique measurements and is an easily observable phenomenon in mercury because of the moderately high vapor density obtainable at low temperatures in the scattering cell. Coherence narrowing results when light radiated by the decay of one atom is absorbed by another in coherent fashion, preserving the phase and orientation of the dipole vibration of the first atom. The newly excited atom then proceeds to precess in the magnetic field in phase with the original atom's precession. If the vapor is dense enough, and the absorption cross sections are fairly large, this process may occur more than once before the radiation finally escapes from the vapor, the apparent lifetime being the sum of the individual lifetimes in each absorption. It has been shown theoretically[12] and experimentally[13] that the coherence-narrowing effect saturates with increasing vapor density, but the ultimate result can be a considerable lengthening of the apparent lifetime.

Eventually (at densities on the order of 10^{14} atoms/cm^3), the familiar "collision broadening"

[10] M. E. Rose and R. L. Carovillano, Phys. Rev. 122, 1185 (1961).

[11] For example, Ref. 3 and some of the articles under Ref. 5; also see B. Budick *et al.*, Phys. Rev. 140, A1041 (1965); W. W. Smith, *ibid.* 137, A330 (1965); H. Bucka *et al.*, *ibid.* 144, 96 (1966).

[12] J. P. Barrat, J. Phys. Radium 20, 541, 633, 657 (1959).

[13] E. B. Salomon and W. Happer, Phys. Rev. 144, 7 (1966).

[14] M. Guiochon, J. E. Blamont, and J. Brossel, J. Phys. Radium 18, 99 (1957).

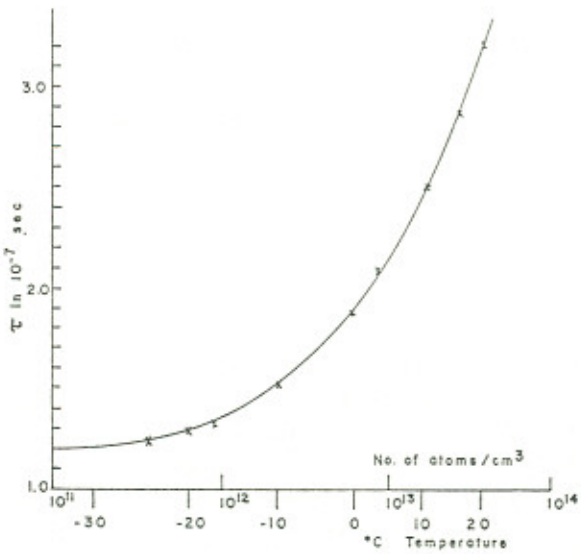

FIG. 3. The effect of coherence narrowing on lifetimes measured at various densities of mercury vapor, taken from Ref. 14. The magnitude of variation of τ with density depends on the size of the vapor-containing bulb—i.e., it is not a true density effect but rather depends on the number of absorbing atoms along the line of observation.

takes precedence over coherence narrowing, and the lifetime shows a rapid decrease with further increase in density. The penetration depth of incident or outgoing resonance radiation is quite small at these densities, however—hence, the Hanle technique is generally not pursued into this region. Figure 3 shows the effects of coherence narrowing only[14] in mercury vapor as a function of temperature. It should be noted that different-size bulbs will show different lifetimes at nonzero temperatures if coherence narrowing is present, because of the different optical path length through the vapor. All sizes of bulbs should show the same extrapolated lifetime at 0°K. It is obvious that errors due to coherence narrowing can be eliminated by taking measurements at several vapor densities and interpolating the resulting curve to zero density.

Finally, it should be pointed out that *non*-coherent trapping of resonance radiation was discovered[15] long before coherent trapping, is of much greater magnitude, and does affect other methods of lifetime measurement (e.g., direct timing techniques). Noncoherent trapping does not affect the Hanle technique, however, except to produce a general depolarization and isotropy of the scattered radiation which decreases the signal-to-background ratio.

Throughout the above discussion, the presence of nuclear spin with the consequent introduction of hyperfine structure splitting has been ignored. In cases where abundant isotopes of nonzero spin are present, the line shape in the Hanle effect can become considerably distorted; and one must either resort to isotopically pure samples or perform a more complex analysis of the line shape obtained. In the case of mercury, the natural admixture of nonzero-spin isotopes is relatively small and may be ignored without serious error.

II. EXPERIMENTAL EQUIPMENT AND TECHNIQUE

Mercury, with a $^1S_0$ ground state, has the experimental advantage of a substantial vapor pressure at room temperature. In addition, good Hg lamps for the production of resonance radiation are readily available. One disadvantage which Hg possesses is that its strongest resonance line ($^1S_0 \leftrightarrow {}^1P_1$) is in the far ultraviolet at 1850 Å. The first forbidden ($^1S_0 \leftrightarrow {}^3P_1$) intercombination transition is a reasonably strong one owing to configuration mixing in mercury, and although still in the ultraviolet at 2537 Å, provides no exceptional difficulties as long as standard quartz optics are used throughout. This transition has a fairly long lifetime, however ($\sim 1 \times 10^{-7}$ sec); hence, the magnetic-field variation required to produce the Hanle effect is quite small, and some care must be taken to buck out stray fields.

As an alternative to the use of mercury, cadmium is a reasonable choice. Cd-vapor lamps made by Osram may be obtained from Ealing or other scientific supply houses, and the much shorter lifetime of 1.6×10^{-9} sec for the $^1P_1 \rightarrow {}^1S_0$ resonance transition at 2288 Å means that one does not need to be fussy about the adjustment of very small compensating magnetic fields, as in the case of mercury (and in fact, all but the main field coils may be dispensed with). Quartz optics will again be necessary through-

[15] Ref. 1, Chap. IV, Sec. 12; M. W. Zemansky, Phys. Rev. 29, 513 (1927).

out the system, and the outer lamp jacket must be removed for transmission of the 2288-Å line. A small oven heated by a gas flame may be used to raise the resonance bulb to the required temperature range of 100°–150°C, the inconvenience of this may be more than compensated for by the much less severe restrictions on magnetic-field compensation and alignment—the choice is left to the reader. For other details of a Cd experiment, see the paper by Lurio and Novick under Ref. 5.

We have built and tested a mercury-resonance experiment as illustrated in Fig. 4. The lamp is an Osram low-pressure mercury lamp, type Hg/3 (available from the Ealing Corp.) with its outer jacket removed for optimum transmission at 2537 Å. The lamp proves to be too noisy and unstable if run from dc or 60-cycle ac. Excitation by rf power at 20–50 MHz eliminates most of the noise problem. We have found a Heathkit Model DX-60A radio transmitter, having about 90 W output and operating in the 10-m band, to be satisfactory. (The lamp typically needs to be started by sparking a Tesla coil near by.) Although the coupling is rather inefficient, adequate rf power may be fed in via coax cable to the standard lamp-socket terminals.

The scattering cell is the only component of the experiment which may cause some difficulty in preparation. Figure 5 shows a suitable design of the "Wood's horn" type, the purpose of the curved taper being to prevent internal back-scattering of the light. The cell must be constructed of quartz in order to pass radiation at 2537 Å. A cylindrical cell would be easier to construct and should be nearly as good if the light enters through a flat end window. (Ready-made cylindrical cells with Vycor bodies and fused silica windows are available from scientific supply houses for use as spectrophotometer cells. These should prove quite usable if the stoppered neck is replaced with a plain neck sealed off under vacuum as described below. We have tried to use the small Hg cell from an Osram lamp as a scattering cell; but even with suitable masking of all but small input and output apertures, we found far too much internal wall scattering which introduced a strong field-independent background, masking the much smaller Hanle signal.) Our cell was prepared on a standard vacuum system with an ultimate pressure of about 10^{-7} mm. The cell was outgassed by thorough heating with a hand torch under vacuum, after which a small amount of Hg was distilled into the cell from a separate side arm, and the cell was then sealed off under the best vacuum obtainable. After this preparation, the cell was coated with flat black paint except for small input and output apertures.

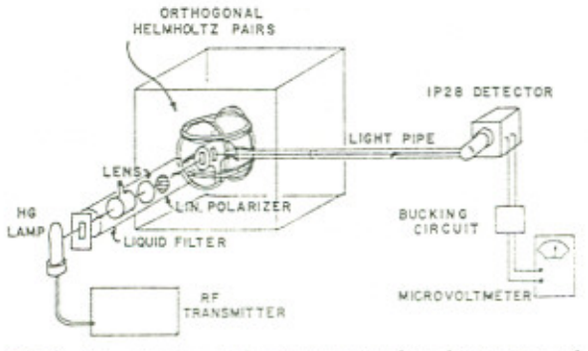

FIG. 4. An experimental arrangement for observation of the Hanle effect.

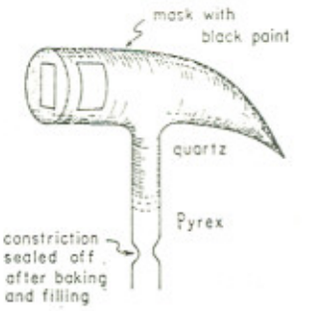

FIG. 5. Design for a "Wood's horn" type of scattering cell.

The half-width at half-maximum of the Lorentzian curve of scattered intensity vs magnetic field is a few tenths of a gauss for the $^3P_1$ state of mercury. This small field necessitates elimination of any transverse field components such as may arise from the ambient earth's field. The apparatus may be aligned so that the z axis coincides with the local earth's field direction, but it will generally be more convenient to use crossed pairs of Helmholtz coils to cancel out various components of the ambient field. Since the bucking coils need produce fields of only a few tenths of a gauss, and the main field coil no more than a gauss or two, they can be quite light in construction. We have used a nested

orthogonal triplet consisting of Helmholts pairs with mean diameters of 23, 19, and 16 cm, which can be conveniently fitted within a light-tight box of reasonable size that also holds the scattering cell. Current may be provided from batteries or small transistor power supplies.

Linear polarizers suitable for use to $\leq$ 2100 Å, and thus suitable for either Hg or Cd, may be obtained from Polacoat, Inc.[16,17] for about $45. It is also quite desirable to use a uv passband filter which will reduce or eliminate unwanted lines from the lamp spectrum. A cheap and highly efficient filter may be made from $CoSO_4$ and $NiSO_4$ mixed with distilled water in the respective portions 5 g, 7 g, 50 cc. (A fairly wide latitude in concentration is permissible.) A filter cell to hold the liquid may be constructed by attaching a small filling arm at right angles to a piece of 3- or 4-cm diam Pyrex tubing, which is then carefully annealed and sawed off on each side of the arm to give a section about 2 cm long. Quartz windows[18] are then attached to the ends with epoxy cement or sealing wax. (We have found a very slow deterioration of filter solutions held in such a cell over periods of months. Fresh fillings appear to be advisable for optimum efficiency.) A filter as described above will pass more than 50% of incident intensity for radiation between 2200 and 3500 Å and less than 1% transmission throughout most of the visible spectrum. Interference filters with much sharper passbands, but also much lower peak transmission (15%–20%) may be obtained from the Baird-Atomic Corp. for about $80.

The detection system consists of a light pipe and a 1P28 photomultiplier tube, the output of which is fed to a microvoltmeter. The photomultiplier tube is affected by small magnetic fields of a few gauss; hence the use of a light pipe 20 or 30 cm long which allows the tube to be somewhat removed from the field region. We have also found the tube to be least sensitive to field changes when placed with its axis at 90° to the field axis. The light pipe is simply constructed by carefully rolling aluminum foil around a glass rod 8 or 10 mm in diam. The aluminum foil is then wrapped with two or three layers of masking tape to stiffen it, and the glass rod is removed. The resulting aluminum tube may be inserted into a glass tube for further protection. The effects of field changes on the photomultiplier may be tested by placing a small dummy scattering surface of black cardboard at the position of the scattering cell. The output current should stay constant as the magnetic field is varied. (The use of a magnetic shield around the tube is apt to distort the field at the scattering cell, unless the tube is kept at some distance, in which case the shield would not be necessary.)

The Hewlett–Packard Model 425A microvoltmeter–ammeter or a similar instrument is convenient for monitoring the output signal from the photomultiplier circuit. We have typically obtained signals having about 30 mV amplitude across a 470-kΩ plate resistor at the collector of the 1P28 photomultiplier, with the latter running at 600 V.

Even with a well-designed scattering cell and careful masking, nonresonant scattering of light can cause a background signal comparable to or larger than the Hanle-effect signal. It is therefore desirable, after minimizing stray scattering, to insert a bucking system in the detector circuit so that the non field-dependent background can be zeroed out. We have found a simple potentiometer circuit consisting of a 10-turn helipot and a small mercury battery in a shielded case, inserted between the photomultiplier and the microvoltmeter, to be quite effective and inexpensive.

Geometric alignment of the polarizer axis and the input and output axes and the adjustment of magnetic-field compensation should all be carried out with some care. The general effect of misalignment is to cause asymmetry in the line shape with respect to reflection about zero field.

Data taking is best accomplished by varying the magnitude of the current supplying the field

---

[16] Polacoat, Inc. 9750 Conklin Road, Blue Ash, Ohio 45242.

[17] M. N. McDermott and R. Novick, J. Opt. Soc. Am. 51, 1008 (1961).

[18] Obtainable in various diameters and thicknesses from Englehard Industries, Inc., Amersil Quartz Division, 685 Ramsey Avenue, Hillside, N. J. Quartz lenses are obtainable from the Farrand Optical Company, Bronx Blvd. and East 238 St., New York, N. Y. at about $19 for a 63-mm-focal-length 39-mm-diam lens.

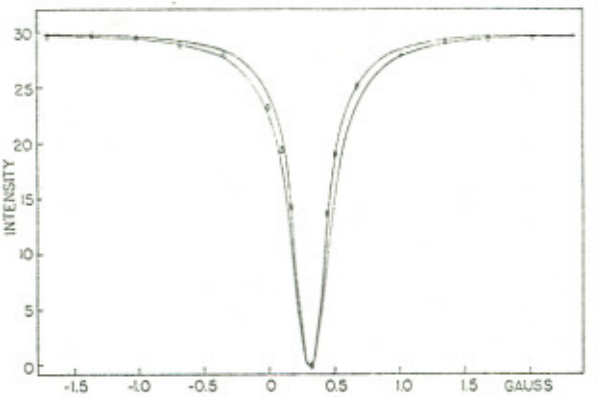

FIG. 6. Data from a typical run taken at 25°C with the apparatus described here. The solid curves represent theoretical Lorentzians corresponding to lifetimes of 2.5 x 10^{-7} and 2.1 x 10^{-7} sec. The ellipses around the data points indicate individual error limits. Field values represent the coil-produced field only, offset by the uncompensated component of the earth's field.

coil and taking sets of readings with the field forward and reversed at each current setting. The resulting curve will, of course, be offset from zero current owing to any uncompensated vertical component of the earth's field.

Since the eye is poor at judging the difference between a Gaussian, Lorentzian, or other bell-shaped curve, it is urged that results be plotted against a family of theoretical Lorentzian curves covering an appropriate range of lifetimes. In that way, any distortions of the curve (e.g., caused by lamp self-reversal) will also be more apparent. Data from a typical run with the apparatus described here are shown in Fig. 6.

In taking measurements at various cell temperatures in order to see coherence narrowing effects, it is important to remember that the coolest part of the cell determines the vapor pressure throughout. Hence, when cooling below room temperature, it is necessary to cool only a small segment of the cell—conversely, when heating above room temperature, all parts of the cell need to be warmed. Cooled or warmed air streams, ice baths, etc., may all be used, as is convenient, for various temperatures.